

Effects of Mixed Herbal Extracts from Parched *Puerariae* Radix, Gingered *Magnoliae* Cortex, *Glycyrrhizae* Radix and *Euphorbiae* Radix (KIOM-79) on Cardiac Ion Channels and Action Potentials

KIOM-79, a mixture of ethanol extracts from four herbs (parched *Puerariae* radix, gingered *Magnoliae* cortex, *Glycyrrhizae* radix and *Euphorbiae* radix), has been developed for the potential therapeutic application to diabetic symptoms. Because screening of unexpected cardiac arrhythmia is compulsory for the new drug development, we investigated the effects of KIOM-79 on the action potential (AP) and various ion channel currents in cardiac myocytes. KIOM-79 decreased the upstroke velocity (V_{max}) and plateau potential while slightly increased the duration of action potential (APD). Consistent with the decreased V_{max} and plateau potential, the peak amplitude of Na^+ current (I_{Na}) and Ca^{2+} current ($I_{Ca,L}$) were decreased by KIOM-79. KIOM-79 showed dual effects on hERG K^+ current; increase of depolarization phase current (I_{depol}) and decreased tail current at repolarization phase (I_{tail}). The increase of APD was suspected due to the decreased I_{tail} . In computer simulation, the change of cardiac action potential could be well simulated based on the effects of KIOM-79 on various membrane currents. As a whole, the influence of KIOM-79 on cardiac ion channels are minor at concentrations effective for the diabetic models (0.1-10 μ g/mL). The results suggest safety in terms of the risk of cardiac arrhythmia. Also, our study demonstrates the usefulness of the cardiac computer simulation in screening drug-induced long-QT syndrome.

Key Words : Heart; Action Potentials; Long-QT Syndrome; Herbal Extract; Ion Channels; hERG

Su Jung Park¹, Kwan Seok Choi¹,
Dong Hoon Shin¹, Jin Sook Kim²,
Dae Sik Jang², Jae Beom Youm³,
Han Choe⁴, Yung E Earm¹, and
Sung Joon Kim^{1,5}

Department of Physiology¹, Seoul National University College of Medicine, Seoul; Department of Herbal Pharmaceutical Development², Korea Institute of Oriental Medicine, Daejeon; National Research Laboratory for Mitochondrial Signaling³, Department of Physiology and Biophysics, Cardiovascular and Metabolic Disease Center, Inje University College of Medicine, Busan; Department of Physiology and Research Institute for Biomacromolecules⁴, University of Ulsan College of Medicine, Seoul; Kidney Research Institute (KRI)⁵, Seoul National University Medical Research Center, Seoul, Korea

Received : 19 May 2008

Accepted : 25 July 2008

Address for correspondence

Sung Joon Kim, M.D.

Department of Physiology, Seoul National University College of Medicine, 28 Yeongeon-dong, Jongno-gu, Seoul 110-799, Korea

Tel : +82.2-740-8230, Fax : +82.2-763-9667

E-mail : sjoonkim@snu.ac.kr

INTRODUCTION

Traditional herbal medicines have been used for the prevention and treatment for diabetes mellitus, which is claimed to be achieved through integrated effects from multiple ingredients (1). Recently, KIOM-79, a mixture of ethanol extracts from four herbs (parched *Puerariae* radix, gingered *Magnoliae* cortex, *Glycyrrhizae* radix and *Euphorbiae* radix) was developed based on the basic known function of each herb in treating diabetes (2-5). Recent studies demonstrate beneficial effects of KIOM-79 on diabetic Goto-Gakizaki rats (6). In the murine macrophages, the inhibition of NF- κ B signaling by KIOM-79 was observed, suggesting an anti-inflammatory action of KIOM-79 (7). Also, KIOM-79 inhibits VEGF expression induced by high glucose or by advanced glycosylation end-products (AGEs) in human retinal pigmented epithelial cells (8).

In the process of therapeutic drug development, promis-

ing candidate compounds are frequently dropped out due to their potential risk of cardiac arrhythmia caused by, for example, K^+ channel inhibition or incomplete inactivation of Na^+ channels (9). Such undesirable effects slow the cardiac repolarization phase, which frequently induces early after-depolarization (EAD). The changes in action potential duration (APD) are usually assessed in terms of the QT interval in the electrocardiogram (ECG). People with inherited mutations of various cardiac ion channels or treated drugs affecting cardiac ion channels show the prolongation of QT interval (long-QT syndrome, LQTS). In severe cases, the afterdepolarization induced by LQTS can trigger fatal arrhythmia, *torsade de pointes*. Although the life-threatening QT prolongation by medical drugs is relatively rare, such risk is obviously unacceptable for novel drug development (9-11). In this respect, traditional herbal medicine should be of no exception for the screening of drug-induced cardiac arrhythmia.

The action potential (AP) of cardiac ventricular myocytes

is divided into five phases. In phase 0, Na⁺ current activation rapidly depolarizes the membrane. The subsequent phase 1 of slight repolarization is followed by a plateau depolarization (phase 2). The phase 2 is due to suppression of inward rectifier as well as the delayed activation of K⁺ currents like IKr and IKs. The termination of phase 2 is caused by the phase 3 repolarization to resting membrane potential, phase 4 (12-14).

The human ether-à-go-go-related gene (hERG) encodes the potassium channel that provides the major repolarizing current early in phase 3 of the cardiac action potential. Inherited LQTS are caused by loss-of-function mutations in several cardiac K⁺ channels like hERG and KCNQ1/mink (LQT1, LQT2), or disrupted fast inactivation of Na⁺ channel, SCN5A (LQT3) (10, 11, 14). In clinical practice, the drug-induced QT prolongation is most commonly caused by direct blockage of hERG channels (9, 11, 14). An incomplete inactivation of Na⁺ channels by drug compounds also causes QT prolongation (10, 15, 16).

In the present study, we investigated the effects of KIOM-79 on hERG channels expressed in HEK-293 cells. Also, we tested in rat cardiac myocytes whether the voltage-activated Na⁺ current and L-type Ca²⁺ current are affected by KIOM-79. Finally, the effects of KIOM-79 on the action potential of rabbit Purkinje fiber were examined and compared with the result of computational simulation of cardiac action potential that reflects the changes of ion channel currents observed in whole-cell patch clamp studies.

MATERIALS AND METHODS

Recording of action potentials

New Zealand White rabbits of either sex were deeply anesthetized with sodium pentobarbitone (50-100 mg/kg, i.p.) for the surgical removal of hearts according to the regulation of Institutional Animal Care and Use Committee (IACUC). Purkinje fibers were isolated from the left ventricles of hearts and mounted in a continuous flow (5 mL/min)-and temperature controlled (37 ± 1°C) chamber superfused with oxygenated normal Tyrode's (NT) solution. The NT solution contained (mM): 143 NaCl, 5.4 KCl, 5 HEPES, 0.33 NaH₂PO₄, 0.5 MgCl₂, 16.6 glucose and 1.8 CaCl₂ at pH 7.4 with NaOH. The tissue was stimulated (2 msec duration and 1.5-2 V amplitude) by silver bipolar electrodes at frequency of 1 Hz to evoke action potentials (APs). APs were recorded using a conventional glass microelectrode with 10-30 MΩ of electrical resistance when filled with 3 M KCl. APs were recorded using Axopatch 1D (Axon Instruments, Foster City, CA, U.S.A.), and data were stored and analyzed using the pClamp 9 (Axon Instruments). Action potential duration at 50% (APD₅₀) and 90% (APD₉₀) of repolarization, resting membrane potential (RMP), total amplitude (TA) of maximum depolarization from RMP, and rate of maximum depolarization at phase 0

(V_{max}) values were analyzed.

Culture of HEK-293 cells expressing hERG channel

HEK293 cells stably expressing the hERG channel, a kind gift from Dr. C. January (17), were cultured in minimum essential medium (MEM) supplemented with 10% fetal bovine serum, 1 mM sodium pyruvate, 0.1 mM nonessential amino acid solution, 100 U/mL penicillin-streptomycin, 100 μg/mL streptomycin sulfate, and 100 μg/mL zeocin in an atmosphere of 95% air and 5% CO₂. At 60-80% confluence, cells were treated with media containing 0.25% trypsin and 0.02% EDTA for 3 min, washed with fresh media, and dispensed to new plastic culture dishes. For electrophysiological recording, cells were trypsinized (30 sec) and moved to recording chamber.

Isolation of rat ventricular myocytes

Young male Sprague-Dawley rats (3 week old) were anesthetized with pentobarbitone sodium (i.p. 200 mg/kg) and injected with heparin (100 U/kg) at the same time. The heart was quickly removed and perfused quickly via the aorta onto a Langendorff retrograde perfusion apparatus. Hearts were initially perfused with NT solution (50 mL), and then perfused with a nominally Ca²⁺ free Tyrode solution (50 mL) containing 0.5 mg/mL of collagenase (Type II, Worthington, U.K.) for 15 min. Finally, this enzyme containing solution was washed out by rinsing with high K⁺, low Cl⁻ storage solution (KB solution) for 5 min. the heart was removed from the Langendorff perfusion apparatus. The ventricular tissues were then agitated and the single cardiac myocytes were isolated and stored in the KB solution at 4°C until used in experiments.

Whole-cell patch clamp

The isolated cells were transferred to a small chamber (0.2 mL) on the stage of an inverted microscope (IX-70, Olympus) and perfused continuously with NT solution at a rate of 10 mL/min. A glass microelectrode with a resistance of 2-2.5 MΩ was used to obtain a gigaohm seal. The conventional whole cell patch clamp technique was used to hold the membrane potential at -60 mV with a patch-clamp amplifier (EPC-9, HEKA elektronik, Germany). For each cell, the capacitance of plasma membrane was automatically analyzed by EPC-9 and used for the normalization of membrane currents. The data were filtered at 5 kHz and displayed on a computer monitor. The data was analysed using Origin (ver. 7.0, Microcal Software, Northampton, MA, U.S.A.). The high-K⁺, low-Cl⁻ storage solution had the following composition (in mM): 70 KOH, 50 L-glutamic acid, 55 KCl, 20 taurine, 20 KH₂PO₄, 3 MgCl₂, 10 glucose, 10 HEPES, 0.5 EGTA at pH 7.3 adjusted with KOH. The pipette solu-

tion for recording K^+ current contained (mM): 100 K^+ aspartate, 25 KCl, 5 NaCl, 10 HEPES, 1 $MgCl_2$, 4 Mg -ATP and 10 1,2-bis(o-aminophenoxy)ethane- N,N,N',N' -tetraacetic acid (BAPTA) at pH 7.2 adjusted with KOH. The pipette solution for recording Ca^{2+} and Na^+ currents (Cs-aspartate internal solution) contained (in mM): 90 Cs-aspartate, 20 CsCl, 2 $MgCl_2$, 5 Mg -ATP, 10 HEPES, 2.5 Na_2 -creatine phosphate, 10 tetraethyl-ammonium chloride (TEA-Cl), 5 Cs-EGTA with pH 7.3 adjusted with CsOH. NT solution was used as the extracellular solution perfusing the experimental bath.

Drugs and chemicals

Preparation of KIOM-79; cortex of *Magnolia officinalis* Rehd. et Wils., radix of *Pueraria lobata* Ohwi, radix of *Glycyrrhiza uralensis* Fisch, and radix of *Euphorbia pekinensis* Ruprecht were collected from the Gansu province in China (2003), and identified by Prof. J.-H. Kim of Division of Life Science of Daejeon University. We deposited all voucher specimens at the herbarium of Korea Institute of Oriental Medicine (Nos. 1240, 2, 7, and 207, respectively). KIOM-79 was prepared as previously described (7). Briefly, equal amounts of gingered Magnoliae cortex, parched Puerariae radix, Glycyrrhizae radix, and Euphorbiae Radix were mixed, pulverized, extracted in 80% EtOH and lyophilized. The 80% EtOH extract was suspended in H_2O (2 L) and successively extracted with *n*-hexane ($\times 3$), EtOAc ($\times 3$), and *n*-BuOH ($\times 3$) to give *n*-hexane, ethyl acetate, *n*-BuOH, and water fractions (174 g), respectively. For experiments, the lyophilized KIOM-79 and its subfractions were dissolved in dimethylsulfoxide (DMSO, 10 mg/mL) with sonication (30 min), and this was used as stock solution. All the other chemicals were purchased from Sigma-Aldrich (St. Louis, MO, U.S.A.).

Statistics

The data is presented as the original recordings and bar graphs of the mean \pm SEM (for *n* tested cells or tissues). Paired or unpaired Student's *t*-test was used for the statistical analysis where appropriate. *P* value <0.05 was considered significant.

RESULTS

The representative trace of membrane potential showed that an application of 10 $\mu g/mL$ of KIOM-79 increased the action potential duration (APD) and slightly decreased the amplitude of AP (Fig. 1A). The effects of KIOM-79 on APD were quantified in terms of APD_{90} and APD_{50} . Also, we measured the V_{max} and TA (see *Materials and methods*). The summarized results from three rabbits showed that TA and V_{max} were decreased by 10 $\mu g/mL$ of KIOM-79. The APD_{90} was

increased by KIOM-79 while APD_{50} was not affected (Fig. 1B). The resting membrane potential (RMP) was not significantly changed by KIOM-79.

The V_{max} and TA are generally regarded to reflect the activity of Na^+ current. Therefore, by using the whole-cell patch clamp technique, we tested the effects of KIOM-79 on the voltage-gated Na^+ current (I_{Na}) in rat ventricular myocytes. To activate I_{Na} selectively without evoking voltage-gated Ca^{2+} current, the holding voltage was clamped at -80 mV and step-like depolarization to -35 mV was applied. By this protocol, a fast inward current was recorded that inactivated almost completely within 10 msec. The activation voltage and kinetics were corresponding with the known properties of voltage-gated Na^+ current (18). An application of KIOM-79 (10 $\mu g/mL$) partially reduced the Na^+ current to 75% of control (Fig. 2).

When the membrane voltage was held at -50 mV, where most of Na^+ channels are inactivated, the step-like depolarizations above -40 mV activated inward currents with relatively slow kinetics of activation and inactivation. The current to voltage relation (*I-V* curve) of the peak inward currents at various test voltages showed an inverted bell-shape (Fig. 3). These properties correspond with the known char-

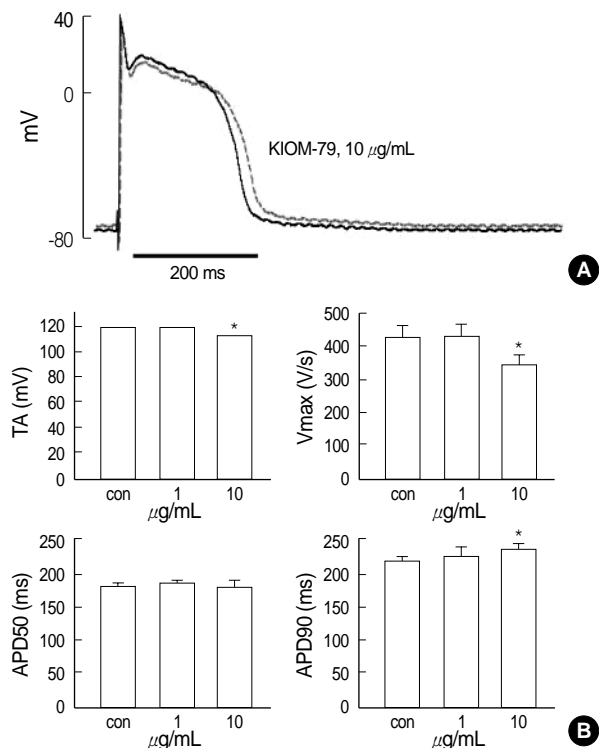


Fig. 1. Effect of KIOM-79 on the APs in rabbit cardiac purkinje fibers. (A) Representative recording of triggered APs in control and in the presence of 10 $\mu g/mL$ KIOM-79 (red trace). (B) Bar graphs showing shortened total amplitude (TA) and rate of maximum depolarization at phase 0 (V_{max}) in the presence of 10 $\mu g/mL$ KIOM-79 (upper panel). APD_{50} was increased by KIOM-79 (10 $\mu g/mL$) while APD_{90} was not affected (lower panels). **P* value <0.05 .

acteristics of L-type Ca^{2+} channels (I_{CaL}) in cardiac myocytes (18). The application of KIOM-79 ($10 \mu\text{g}/\text{mL}$) also decreased the amplitudes of Ca^{2+} current (I_{Ca}) by about 20% (Fig. 3).

The increase of APD_{90} , i.e. delayed repolarization, in AP

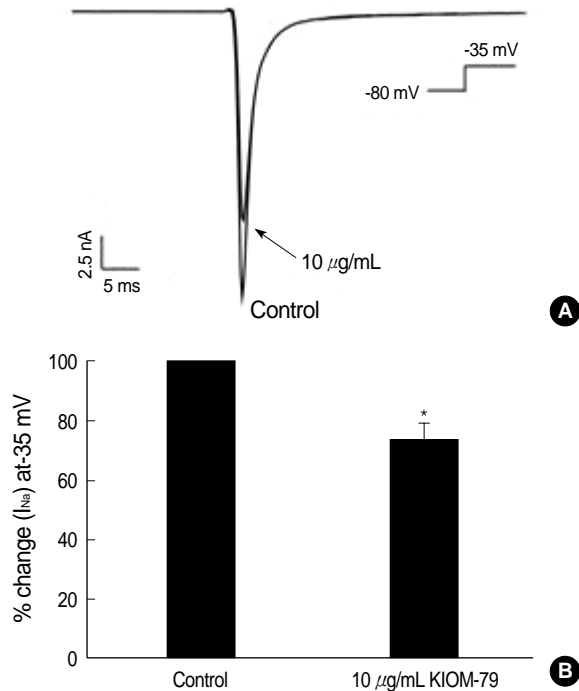


Fig. 2. Effect of KIOM-79 on voltage-gated Na^+ current (I_{Na}) in rat ventricular myocytes. (A) A representative trace of membrane currents in rat ventricular myocytes obtained with Cs^+ pipette solution. A transient I_{Na} was activated with a test depolarization (-35 mV) from holding potential of -80 mV . The I_{Na} was decrease by $10 \mu\text{g}/\text{mL}$ KIOM-79 (arrow). (B) Summary of the effects of KIOM-79 on the peak amplitude of I_{Na} . In each cell, the current amplitudes measured at the peak of current were normalized to the control amplitude and mean \pm SEM values were plotted ($n=6$). * P value < 0.05 .

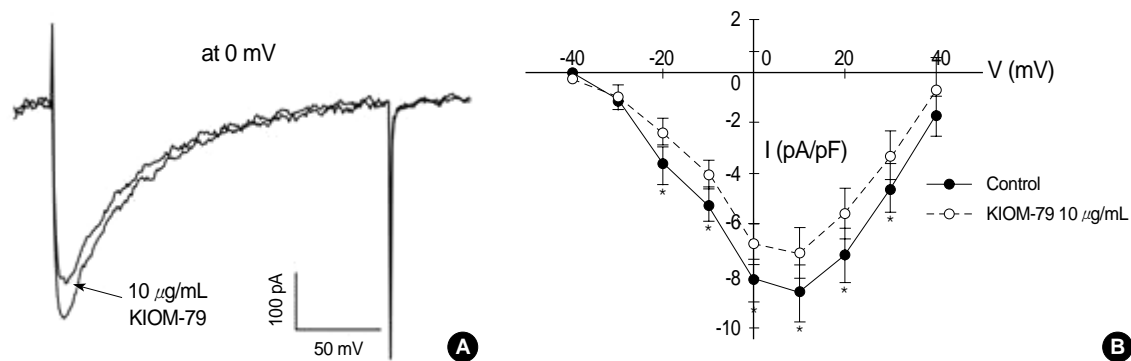


Fig. 3. Effect of KIOM-79 on voltage-gated L-type Ca^{2+} current (I_{CaL}) in rat ventricular myocytes. (A) The inward currents were recorded in rat ventricular myocytes with the Cs^+ pipette solution. A representative current obtained by depolarizing pulse from -50 to 0 mV (200 msec) is shown. KIOM-79 ($10 \mu\text{g}/\text{mL}$) slightly decreased the inward current. (B) To obtain the I-V curve of I_{CaL} , the membrane voltage was held at -50 mV and incremental step-like pulses were from -40 to 40 mV (10 mV intervals, 200 msec duration). The amplitudes of I-V curves were decreased by $10 \mu\text{g}/\text{mL}$ KIOM-79. Each symbol represents mean \pm SEM of current amplitudes normalized to the cell capacitance (pA/pF , $n=5$). * P value < 0.05 .

recordings suggested that K^+ channels might have been inhibited by KIOM-79. Since the cardiac action potential of rabbit is relatively short ($200\text{--}250 \text{ msec}$), I_{Kr} is the predominant player for repolarization (13, 14). To get precise quantitative evaluation of I_{Kr} , we tested the effects of KIOM-79 on hERG channels expressed in HEK293 cells. In the whole-cell patch clamp recording with K^+ pipette solution, the membrane voltage was depolarized from -80 to 20 mV (1 sec) and then repolarized to -50 mV (1 sec). Fig. 4A shows an example of representative current traces both under control conditions and after exposure to $10 \mu\text{g}/\text{mL}$ KIOM-79. The depolarizing step pulse (20 mV) activated a time-dependent outward current (I_{depol}) that was increased by KIOM-79. However, the increasing effect on I_{depol} was significant only at relatively low concentration of KIOM-79 (Fig. 4B). During the repolarization phase (-50 mV), a transient outward current larger than I_{depol} was measured, and the peak amplitude of this 'tail current' (I_{tail}) was decreased by KIOM-79. Fig. 4B shows a dose-dependent effect of KIOM-79 ($0.01\text{--}100 \mu\text{g}/\text{mL}$) on I_{depol} and I_{tail} . With $10 \mu\text{g}/\text{mL}$ of KIOM-79, the decrease of I_{tail} was only partial (70%), and this was not different from the decrease induced by $100 \mu\text{g}/\text{mL}$ of KIOM-79. The increasing effect on I_{depol} was statistically significant only at $1 \mu\text{g}/\text{mL}$ (paired t-test).

We also examined the effects of KIOM-79 on hERG current at different voltages. The amplitude of I_{depol} was normalized to the membrane area (pA/pF). The current-voltage relation (I/V curve) of I_{depol} showed a bell-shape, a well-known property of hERG (Fig. 4C). The averaged I-V curve for I_{depol} obtained at $10 \mu\text{g}/\text{mL}$ of KIOM-79 is also plotted in Fig. 4C. The increase of I_{depol} by KIOM-79 was observed throughout the test voltages from above -10 mV . The mean amplitudes of normalized I_{tail} (pA/pF) measured at the common repolarization voltage (-50 mV) after various levels of depolarizing voltages were plotted in Fig. 4D. The I-V curve of I_{tail} shows a voltage-dependent activation of hERG channels that reached

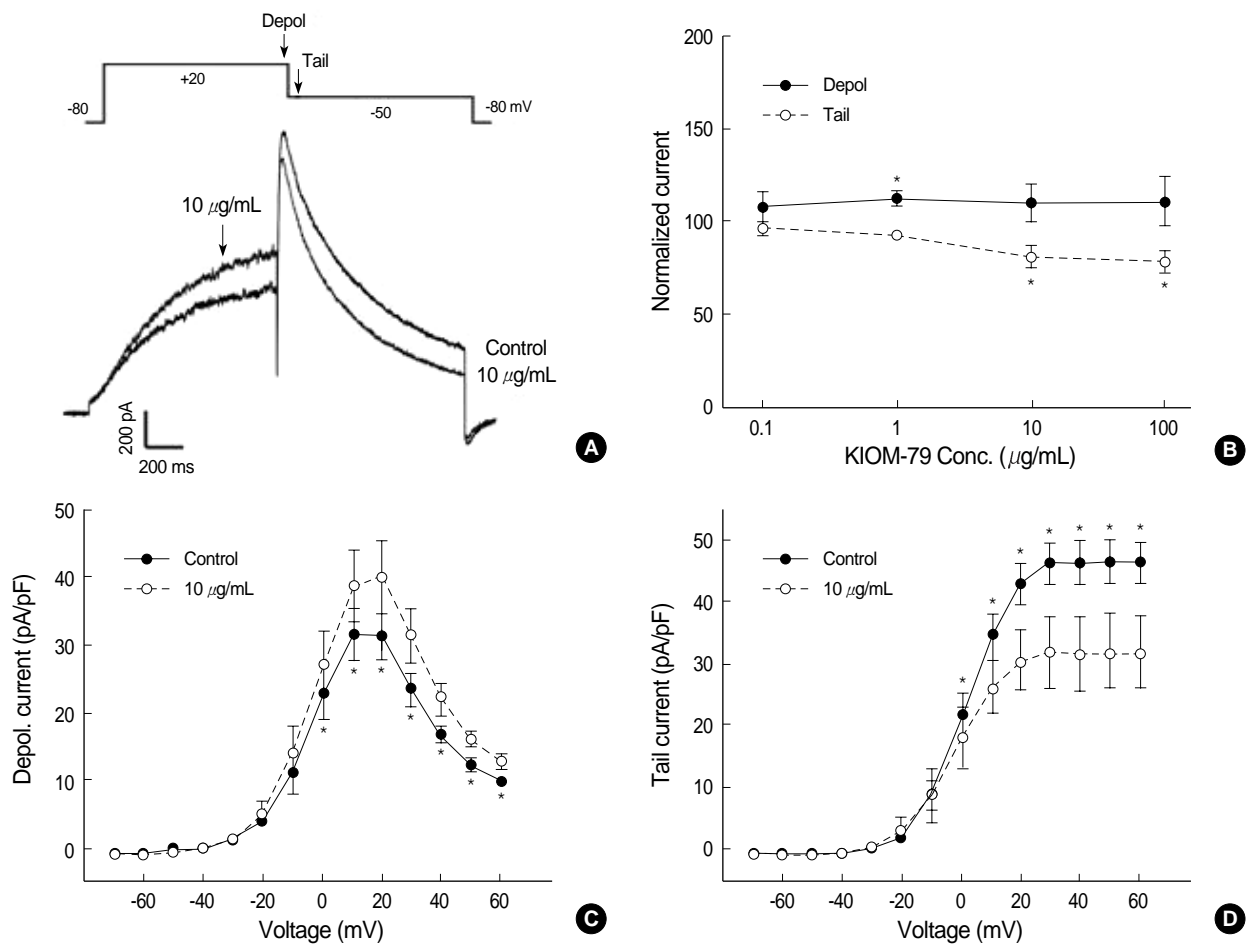


Fig. 4. Effects of KIOM-79 on hERG current. (A) Representative hERG current traces recorded from HEK293 cells before and after application of 10 μg/mL KIOM-79. The currents were recorded with a test depolarization from the holding potential of -80 to +20 mV (1 sec), with tail currents recorded upon repolarization to -50 mV for 1 sec. (B) Dose dependent relationship for the increase of I_{depol} (●) and the decrease of I_{tail} (○) by KIOM-79 (μg/mL): 0.1 (n=3), 1 (n=8), 10 (n=10), 100 (n=5). Each symbol represents mean ± SEM of current amplitudes normalized to control currents (%). The amplitudes of I_{depol} and I_{tail} were measured at the timing indicated by downward arrows in the pulse protocol of panel (A). (C, D) I-V curves for I_{depol} and I_{tail} before and after application of 10 μg/mL KIOM-79. Each symbol represents mean ± SEM of current amplitudes normalized to the cell capacitance (pA/pF, n=6). *P value <0.05 vs. control.

a steady-state at +30 mV. The partial decrease of I_{tail} by KIOM-79 (10 μg/mL) was observed from above 0 mV.

Because KIOM-79 seemed to have multiple effects on hERG current, we further tested the effects of KIOM-79 fractions divided by their polarity; water soluble fraction, butanol fraction, ethylacetate fraction, and hexane fraction. The water fraction showed no effect on hERG current (Fig. 5A) whereas the butanol and hexane fraction exerted both I_{depol} increase and I_{tail} decrease (Fig. 5B, D). Interestingly, the ethylacetate fraction selectively increased the I_{depol} without affecting the amplitude of I_{tail} (Fig. 5C).

As a whole, the decreased I_{tail} of hERG was consistent with the increase of APD₉₀, and the decrease of I_{Na} and I_{CaL} could explain the decrease of V_{max} and TA by KIOM-79. However, it was not clear whether the increase of I_{depol} amplitude in hERG by KIOM-79 has affected the shape of AP. Also, the quantitative correlation between changes of individual cur-

rent system and the overall effects on AP are not clear. To get a speculation on this question, we exploited a computerized electrophysiology model of rabbit ventricular myocytes.

The computer simulation model used in this study is mostly based on Kyoto model (19). Since the Kyoto model was originally constructed based on the data from guinea-pig ventricle, we modified the model to fit the experimental data from rabbit ventricle. This model contains many kinds of ion channel including hERG (I_{Kr}), Na^+ channel (I_{Na}) and Ca^{2+} channel (I_{CaL}). The mathematical representative of hERG is as follows.

$$I_{hERG} = G_{hERG} \cdot C_m \cdot (V_m - E_K) \cdot (0.1 \cdot m_1 + 0.9 \cdot m_2) \cdot h$$

$$G_{hERG} = 0.3024 \cdot (K_o / 5.4)^{0.2}$$

$$C_m = 132 \text{ pF}, K_o = 142 \text{ mM}$$

$$\alpha_{m1} = 1 / \{20 \cdot \exp(-V_m / 11.5) + 5.0 \cdot \exp(-V_m / 300)\}$$

$$\beta_{m1} = 1 / \{160 \cdot \exp(V_m / 28.0) + 200 \cdot \exp(V_m / 1,000.0)\} + 1 /$$

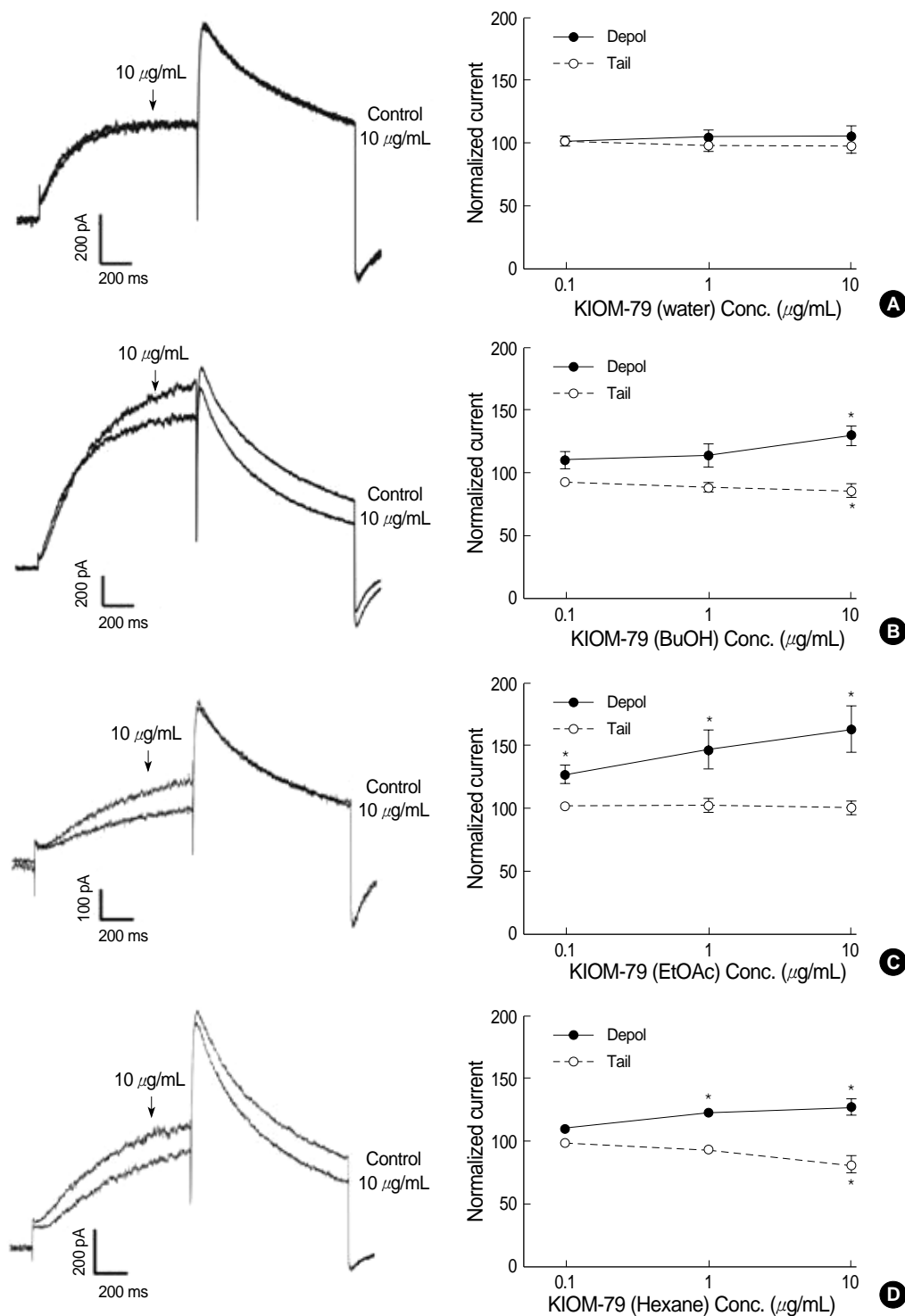


Fig. 5. Effects of the three different fractions of KIOM-79 on hERG current. Left panels; representative current traces obtained by step like pulses same as Fig. 4A. Right panels; dose dependent relationships for I_{depol} (closed circle) and I_{tail} (open circle). (A) No significant effect of the water extract ($n=6$). (B) Effects of butanol (BuOH) fraction demonstrating the increase of I_{depol} and the decrease of I_{tail} ($n=5$). (C) Effects of ethylacetate (EtOAc) fraction demonstrating the increase of I_{depol} while no effect on I_{tail} ($n=6$). (D) Effects of hexane fraction demonstrating the increase of I_{depol} and the decrease of I_{tail} ($n=6$). Each symbol represents mean \pm SEM of current amplitudes normalized to control currents (%). * P value <0.05 vs. control.

$$(2500 \cdot \exp(V_m/20))$$

$$\alpha_{m2} = 1 / \{1,333 \cdot \exp(-V_m/13) + 133.3 \cdot \exp(-V_m/300)\}$$

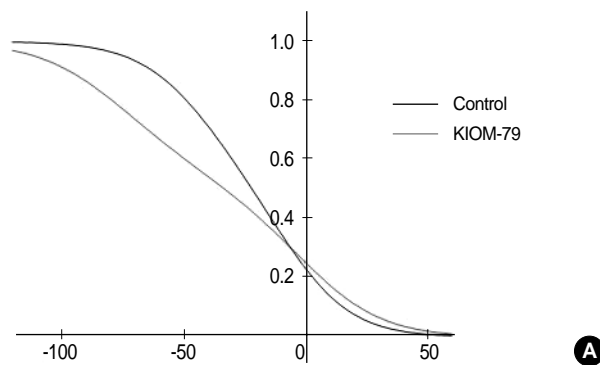
$$\beta_{m2} = 1 / \{10,666 \cdot \exp(V_m/28) + 13,333 \cdot \exp(V_m/1,000)\} + 1 / (10,000 \cdot \exp(V_m/20))$$

$$\alpha_h = 3.5 / \{5.6 \cdot \exp(V_m/15) + 2.4 \cdot \exp(V_m/300)\}$$

$$\beta_h = 1 / \{0.067 \cdot \exp(-V_m/15) + 0.63 \cdot \exp(-V_m/150)\}$$

Symbols	Definition
I_{HERG}	hERG current (pA)
G_{HERG}	Maximum conductance of hERG (nS)
m_1, m_2	Two components of activation gate of hERG
h	Inactivation gate of hERG
α_x	Opening rate constant of gate x (/msec)
β_x	Closing rate constant of gate x (/msec)
C_m	Membrane capacitance (pF)
V_m	Membrane potential (mV)
E_K	Equilibrium potential for K^+ (mV)
K_o	Concentration of K^+ outside of the cell (mM)

Among the parameters describing the kinetics of hERG activation and inactivation, a modification of parameters related to inactivation was crucial to the reproducing the effects of KIOM-79 on hERG current. To mimic the changes of recorded hERG current by KIOM-79, we shifted the voltage-dependence of opening and closing rate constants related with the inactivation process to the right by 10 mV and to the left by 30 mV, respectively. By this, the voltage-dependence of steady-state inactivation was reduced (Fig. 6A), and the dual effects of KIOM-79 on I_{depol} at 20 mV and on I_{tail} at -50 mV were reproduced (Fig. 6B) similar with the record-



ings shown in Fig. 4A.

As we applied these changes in parameters (i.e. the shift of voltage-dependence of opening and closing rate constants of hERG) to the computational model of AP, it was found that APD₉₀ was prolonged similar to the recording of APs (Fig. 7A). In Fig. 7A, the peak amplitude of AP and V_{max} were also slightly decreased because the conductance of Na^+ current was decreased by 25% reflecting the recorded decrease of I_{Na} . In the simulated result of Fig. 7A, however, the slight decrease of plateau level shown in Fig. 1A was not reproduced. The disparity was further resolved by considering the effect of KIOM-79 on the amplitude of I_{CaL} . As we additionally reduced the conductance of I_{CaL} to 85% of control, the plateau of reconstituted AP (Fig. 7B) was found to be lowered similar to that shown in Fig. 1A. The degree of prolongation in APD, however, became slightly smaller than the simulated result in Fig. 7A.

DISCUSSION

In cardiac APs, the key players of phase 3 repolarization are I_{Kr} (rapid delayed rectifier K^+ current) and I_{Ks} (slow delayed rectifier K^+ current) conducted by hERG/KCNE2 and KCNQ/minK, respectively (10, 12, 13). However, in the experimental animals like rabbit, the contribution of I_{Ks} seems minor because the durations of cardiac APs are relatively short (200–250 ms).

The initial aim of this study was to evaluate the risk of KIOM-79 on cardiac action potential, i.e. drug-induced AP

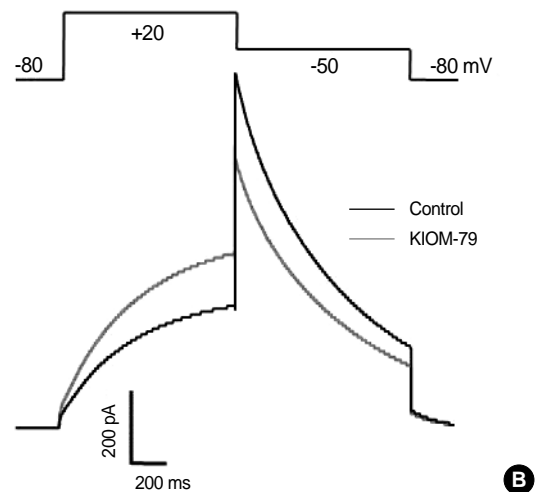


Fig. 6. Computer simulation of the effects of KIOM-79 on the voltage-dependence of hERG channel activity. (A) A proposed change in voltage-dependence of steady-state inactivation of hERG to reproduce the effects of KIOM-79 on hERG current in Fig. 4. In

order to reduce the slope of the voltage-dependence of steady-state inactivation, the opening and closing rate constants were modified as follows. $\alpha_h = 1.0 / \{1.6 \cdot \exp([V_m - 10] / 17.0) + 0.7 \cdot \exp([V_m - 10] / 300.0)\}$; $\beta_h = 1.0 / \{0.067 \cdot \exp(-[V_m + 30] / 17.0) + 0.63 \cdot \exp(-[V_m + 30] / 150.0)\}$. The voltage-dependence of opening rate constant was shifted to the right by 10 mV, while that of closing rate constant was shifted to the left by 30 mV. Note that the voltage-dependence shows a deviation from typical Boltzman distribution since there are two exponential terms in the equations describing α_h and β_h . (B) Reconstructed hERG currents from the altered rate constants of inactivation. Altered inactivation increased the amplitude of membrane current activated by a depolarizing step from -80 mV to +20 mV, whereas it reduced the amplitude of membrane current activated by a repolarizing step from +20 to -50 mV.

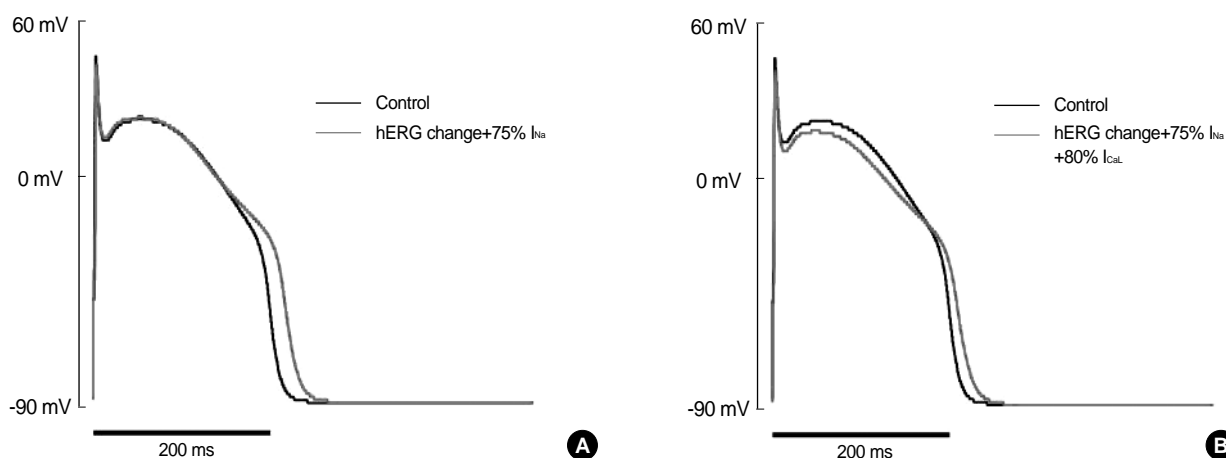


Fig. 7. Computer simulation of the changes in AP shape by altered properties of hERG, I_{Na} and I_{CaL} channels. (A) Changes in AP shape by applying the altered inactivation of hERG (Fig. 6) and the decrease in Na^+ -channel density (75% of control) to the computational model. By this modification, the APD_{50} of reconstructed action potential was prolonged from 208.7 to 230.7 msec, and the peak amplitude of phase 0 was decreased, similar with the results from Fig. 1. (B) When the conductance of I_{CaL} was reduced (80% of control) in addition to the above changes in hERG and I_{Na} , the plateau potential was also affected reproducing the results from the cardiac Purkinje fiber of rabbits. The degree of prolongation in APD_{50} ($\Delta APD_{50}=15.5$ ms) was rather small compared with the results ($\Delta APD_{50}=22.0$ msec) in (A).

lengthening. Actually, the decrease of I_{tail} in hERG suggested such possibility. However, as was found in the AP measurement and also in the computer simulation, the moderate changes of hERG current induced by KIOM-79 is reflected as only weak changes of AP. Because the change in hERG amplitude was already saturated at $10 \mu\text{g/mL}$, it is suggested that the risk of AP lengthening and early afterdepolarization by KIOM-79 would be relatively low.

The complex effects of KIOM-79 on hERG, i.e. increase of I_{depol} and decrease of I_{tail} , were intriguing. Nevertheless, such complexity was not surprising considering that multiple compounds are likely to be present in this extract. The test of fractions of KIOM-79 suggested that the dual effects of KIOM-79 might be partially separated depending on the differential solubility to organic solvents display similar effects on hERG. Since the water fraction had no effect, we could exclude the polysaccharide compounds as the candidate acting on hERG channel. The hexane fraction showed dual effects, i.e. increased I_{depol} and decreased I_{tail} , similar with those of KIOM-79. The butanol fraction also showed the dual effects, however, the increase of I_{depol} was significant only at $10 \mu\text{g/mL}$. The ethylacetate fraction only increased I_{depol} , and this effect was quite potent (P value <0.05 at $0.1 \mu\text{g/mL}$).

Solvent fractionation is a method to separate compounds based on their relative solubilities in two different immiscible liquids, usually water and an organic solvent. The order of polarity between the above four fractions is water (1.0) >butanol (0.602) >ethylacetate (0.228) >hexane (0.009). Generally, therefore, the petroleum ether or *n*-hexane fraction contains non-polar compounds like lipids, fatty acids, essential oils, steroids or triterpenoids. The ethyl acetate fraction has higher portion of polar components than petroleum ether or

n-hexane fraction. The *n*-BuOH fraction contains polar compounds, mainly glycosides and tannins. Evaporation of the remaining water layer leaves polar glycosides, sugars, organic acids as a viscous gum (19, 20). However, separation by solvent partitioning cannot be always performed in a clearcut manner; overlapping of the compounds in successive fractions is usually found (19, 21). In the present study, the dual effects on hERG current were commonly observed, although the potency is different, in butanol and hexane fractions. Such overlapping results might be due to the incomplete separation of effective components. Otherwise, it might suggest that multiple compounds exert similar effects on hERG channels.

In the whole-cell patch clamp recordings of isolated cardiac myocytes, we also found that the peak amplitude of I_{Na} was decreased by KIOM-79. However, due to the huge conductance of Na^+ channels when during the upstroke phase (phase 0) of cardiac AP (reference), a partial decrease of I_{Na} (about 75% of control) induced only a slight decrease of TA and upstroke velocity (V_{max}). The slight decrease of plateau potential might be due to either the decrease of I_{Ca} or the slight increase of hERG current in its depolarizing phase (I_{depol}).

The screening of drug molecules for their adverse effects on cardiac ion channels is demanding but becoming accelerated by the development of automated patch clamp systems (9). Compared with the patch clamp recording, the reliable recording of cardiac action potential in the isolated tissues like Purkinje fiber is technically demanding and requires cumbersome procedure. In this respect, the application of computerized model of cardiac action potential combined with patch clamp data might provide an efficient tool to save the cost of cardiac toxicity screening of drug development (22, 23). This could be also valid in traditional herbal drugs

where numerous effects from multiple compounds are anticipated. In this study, we confirmed satisfactory consistence of the simulated results from virtual rabbit cardiomyocyte model combined with patch clamp study and the real conventional electrode recording. Our present results might imply the potential usefulness of the computational modeling in cardiac electrophysiology.

As mentioned above, KIOM-79 is a mixture of extracts from four herbs; parched *Puerariae* radix, gingered *Magnoliae* cortex, *Glycyrrhiza* radix and *Euphorbiae* radix. Literature search shows that puerarin from *Puerariae* partially inhibits L-type Ca^{2+} channels and cardiac Na^{+} current (25, 26), which might explain the partial inhibition of I_{Ca} and I_{Na} by KIOM-79. Also, magnolol from *Magnoliae* cortex shows ion channel regulatory effects on maxi- K^{+} channel and Ca^{2+} channels in smooth muscle and NMDA receptors in neuronal cells (27-29). However, no previous studies have directly tested these compounds on cardiac ion channels and APs.

In summary, in this study, we examined the effect of KIOM-79 on cardiac ion channels that play critical roles in determining the parameters of APs. Partial inhibitory effects on hERG current and I_{Na} induced increase of APD_{90} and decrease of V_{max} , respectively. However, such changes are relatively minute and do not cause afterdepolarization. Because less than 1 $\mu\text{g}/\text{mL}$ of KIOM-79 can effectively inhibit VEGF expression and MAPK activity (8), only a moderate change of cardiac AP by 10 $\mu\text{g}/\text{mL}$ of KIOM-79 suggests relative safety in terms of the drug-induced long QT syndrome in cardiac electrophysiology.

REFERENCES

- Li WL, Zheng HC, Bukuru J, De Kimpe N. *Natural medicines used in the traditional Chinese medical system for therapy of diabetes mellitus*. *J Ethnopharmacol* 2004; 92: 1-21.
- Aida K, Tawata M, Shindo H, Onaya T, Sasaki T, Yamaguchi T, Chin M, Mitsuhashi H. *Isoliquiritigenin: a new aldose reductase inhibitor from glycyrrhizae radix*. *Planta Medicine* 1990; 56: 254-8.
- Alarcon-Aguilara FJ, Roman-Ramos R, Perez-Gutierrez S, Aguilar-Contreras A, Contreras-Weber CC, Flores-Saenz JL. *Study of the anti-hyperglycemic effect of plants used as antidiabetics*. *J Ethnopharmacol* 1998; 61: 101-10.
- Hur J. *Donguibogam Parallel Version*. Committee of Dongui Bogam Translation. Bupin Publishes Co., Seoul, Korea, 1999.
- Kang KA, Chae S, Koh YS, Kim JS, Lee JH, You HJ, Hyun JW. *Protective effect of puerariae radix on oxidative stress induced by hydrogen peroxide and streptozotocin*. *Biol Pharm Bull* 2005; 28: 1154-60.
- Kim CS, Sohn EJ, Kim YS, Jung DH, Jang DS, Lee YM, Kim DH, Kim JS. *Effects of KIOM-79 on hyperglycemia and diabetic nephropathy in type 2 diabetic Goto-Kakizaki rats*. *J Ethnopharmacol* 2007; 111: 240-7.
- Jeon YJ, Li MH, Lee KY, Kim JS, You HJ, Lee SK, Sohn HM, Choi SJ, Koh JW, Chang IY. *KIOM-79 inhibits LPS-induced iNOS gene expression by blocking NF-kappaB/Rel and p38 kinase activation in murine macrophages*. *J Ethnopharmacol* 2006; 108: 38-45.
- Kim YS, Jung DH, Kim NH, Lee YM, Jang DS, Song GY, Kim JS. *KIOM-79 inhibits high glucose or AGEs-induced VEGF expression in human retinal pigment epithelial cells*. *J Ethnopharmacol* 2007; 112: 166-72.
- Netzer R, Ebnet A, Bischoff U, Pongs O. *Screening lead compounds for QT interval prolongation*. *Drug Discov Today* 2001; 6: 78-84.
- Marban E. *Cardiac channelopathies*. *Nature* 2002; 415: 213-8.
- Roden DM. *Clinical practice. Long QT syndrome*. *New Engl J Med* 2008; 358: 169-76.
- Schram G, Pourrier M, Melnyk P, Nattel S. *Differential distribution of cardiac ion channel expression as a basis for regional specialization in electrical function*. *Circ Res* 2002; 90: 939-50.
- Cheng JH, Kodama I. *Two components of delayed rectifier K^{+} current in heart: molecular basis, functional diversity, and contribution to repolarization*. *Acta Pharmacol Sin* 2004; 25: 137-45.
- Sanguinetti MC, Tristani-Firouzi M. *hERG potassium channels and cardiac arrhythmia*. *Nature* 2006; 440: 463-9.
- Yuill KH, Convery MK, Dooley PC, Doggrell SA, Hancox JC. *Effects of BDF 9198 on action potentials and ionic currents from guinea-pig isolated ventricular myocytes*. *Br J Pharmacol* 2000; 130: 1753-66.
- Yoon JY, Ahn SH, Oh H, Kim YS, Ryu SY, Ho WK, Lee SH. *A novel Na^{+} channel agonist, dimethyl lithospermate B, slows Na^{+} current inactivation and increases action potential duration in isolated rat ventricular myocytes*. *Br J Pharmacol* 2004; 143: 765-73.
- Zhou Z, Gong Q, Ye B, Fan Z, Makielski JC, Robertson GA, January CT. *Properties of hERG channels stably expressed in HEK 293 cells studied at physiological temperature*. *Biophys J* 1998; 74: 230-41.
- Hille B. *Ion Channels of Excitable Membranes*. 3rd Ed. Sunderland, MA: Sinauer Associates 2001.
- Woo WS. *Methods in Natural Product Chemistry*. Seoul: Seoul National University Press, 2002; 12-3.
- Zhang Y, Chen J, Zhang C, Wu W, Liang X. *Analysis of the estrogenic components in kudzu root by bioassay and high performance liquid chromatography*. *J Steroid Biochem Mol Biol* 2005; 94: 375-81.
- Otsuka H. *Purification by Solvent Extraction Using Partition Coefficient*. In: Sarker SD, Latif Z, Gray AI, editors, *Methods in Biotechnology*. Vol. 20 Natural Products Isolation, 2nd Ed. Totowa, NJ: Humana Press 2005; 269-73.
- Matsuoka S, Sarai N, Kuratomi S, Ono K, Noma A. *Role of individual ionic current systems in ventricular cells hypothesized by a model study*. *Jpn J Physiol* 2003; 53: 105-23.
- Sarai N, Matsuoka S, Noma A. *simBio: a Java package for the development of detailed cell models*. *Prog Biophys Mol Biol* 2006; 90: 360-77.
- Meyer T, Sartipy P, Blind F, Leisgen C, Guenther E. *New cell models and assays in cardiac safety profiling*. *Expert Opin Drug Metab Toxicol* 2007; 3: 507-17.
- Qian Y, Li Z, Huang L, Han X, Sun J, Zhou H, Liu Z. *Blocking effect of puerarin on calcium channel in isolated guinea pig ventricular myocytes*. *Chin Med J (Engl)* 1999; 112: 787-9.

26. Zhang GQ, Hao XM, Dai DZ, Fu Y, Zhou PA, Wu CH. *Puerarin blocks Na⁺ current in rat ventricular myocytes.* *Acta Pharmacol Sin* 2003; 24: 1212-6.
27. Lin YR, Chen HH, Ko CH, Chan MH. *Differential inhibitory effects of honokiol and magnolol on excitatory amino acid-evoked cation signals and NMDA-induced seizures.* *Neuropharmacology* 2005; 49: 542-50.
28. Liu YC, Lo YC, Huang CW, Wu SN. *Inhibitory action of ICI-182,780, an estrogen receptor antagonist, on BK(Ca) channel activity in cultured endothelial cells of human coronary artery.* *Biochem Pharmacol* 2003; 66: 2053-63.
29. Wu SN, Chen CC, Li HF, Lo YK, Chen SA, Chiang HT. *Stimulation of the BK(Ca) channel in cultured smooth muscle cells of human trachea by magnolol.* *Thorax* 2002; 57: 67-74.